

# SAR image change detection method based on PPNN

Guoli NIE<sup>1,2</sup>, Guisheng LIAO<sup>1,2,3</sup> & Cao ZENG<sup>2,3,4\*</sup>

<sup>1</sup>National Laboratory of Radar Signal Processing, Xidian University, Xi'an 710071, China;

<sup>2</sup>International Cooperation Base of Integrated Electronic Information System of Ministry of Science and Technology, Xidian University, Xi'an 710071, China;

<sup>3</sup>2011 Collaborative Innovation Center of Information Sensing, Xidian University, Xi'an 710071, China;

<sup>4</sup>Radar Cognitive Detection, Imaging and Target Recognition Overseas Expertise Introduction Center for Discipline Innovation ("111 Center"), Xidian University, Xi'an 710071, China

Received 12 October 2019/Revised 13 December 2019/Accepted 30 March 2020/Published online 7 July 2021

**Citation** Nie G L, Liao G S, Zeng C. SAR image change detection method based on PPNN. *Sci China Inf Sci*, 2021, 64(8): 189304, https://doi.org/10.1007/s11432-019-2865-5

Dear editor,

In remote sensing research, change detection is said to be a hot spot because of its many applications [1], and lots of synthetic aperture radar (SAR) image change detection methods are proposed. In this study, to address the problem that the accuracy of SAR image change detection needs to be improved, a multi-feature parallel probabilistic neural network (PPNN) is proposed.

Probabilistic neural network (PNN) is a feedforward neural network, which is widely used in several fields of image classification [2]. In PNN [3], the probability of the pixel point belonging to a certain class is obtained by calculating the sum of the Euclidean distances of a single pixel point and two types of sample points, and the category with the high probability is selected as the pixel point. The method extends the clustering problem of pixels from the point-to-point relationship to the connection between points and a set of points. In the PPNN, two networks are connected in parallel, and the difference image (DI) of two different features formed by two different DI generation operators is inputted and the probability of pixel point belongs to the change class, or the non-change class can be calculate as  $a_1$  and  $b_1$  ( $a_1 + b_1 = 1$ ). If  $a_1 + a_2 > b_1 + b_2$ , it implies that under different DI features, the comprehensive probability of this pixel point that belongs to the change class is larger. In the PPNN, the nodes corresponding to the two PNN summation layers are connected to the nodes of the second layer and weighted and summed. The node values of the second summation layer are compared to classify the pixels of the original DI. The DI operators in this study are log ratio and mean ratio, which are widely used in change detection.

**Structure of PPNN.** The structure of PPNN is shown in Figure 1(a). As can be seen in Figure 1(a), the PPNN is divided into five layers. The first layer is the input layer, which is used to receive the input data, multiply it by a certain weight  $w_i$ , and then import it to the next layer. The number of input layer nodes is equal to the dimension of

the input vector. Since the change detection focuses on the change of a single pixel and for SAR images, the value of each pixel point is independent of its position in the image, so  $w_i = 1$  can be set.

The second layer is the pattern layer. In this layer, first, the Euclidean distance of each input pixel and all nodes of the mode layer is obtained, that is,  $m$  Euclidean distances  $D$  are obtained at this time, and then substituted into the activation function  $e^{-D}$  of the pattern layer and  $D = |x_{ij} - t_{ij}|$ , where  $t_{ij}$  represents the  $j$ th pixel sample in the  $i$ th single network. The number of nodes in the pattern layer is equal to the number of sample pixel.

The summation layer 2 has two nodes, which are individually connected to the nodes of the same half of the summation layers of the two PNNs (called the summation layer 1 in the PPNN). The summation layer 2 weights the nodes of the corresponding categories of the two PNNs, which the obtained values are, respectively, located at the two nodes of it, and then compares the numerical values in the two nodes. That is,  $P_1 = C_{11} + WC_{21}$ ,  $P_2 = C_{12} + WC_{22}$ ; if  $P_1 > P_2$ , then the pixel point  $x_i$  is considered part of the category indicated by  $P_1$ .

The last layer is the output layer, and its role is to judge the probability, with outputs 1 and 0.

**Our method.** First, the two DI image matrices ( $m \times n$ ) are transformed into two one-dimensional matrices ( $1 \times m \times n$ ) and then are imported into the input layer. Second, the network passes each node of the input layer to all nodes of the pattern layer at the same time and then calculates the pixel difference value at the node of each pattern layer. Third, all the differences are substituted using the Bayes' theorem formula, which is described as

$$p(x|W_i) = \frac{1}{N_i} \sum_{k=1}^{N_i} \frac{1}{(\sqrt{2\pi}\sigma^2)^d} \exp\left(-\frac{\|x - x_{ik}\|^2}{2\sigma^2}\right), \quad (1)$$

\* Corresponding author (email: czeng@mail.xidian.edu.cn)

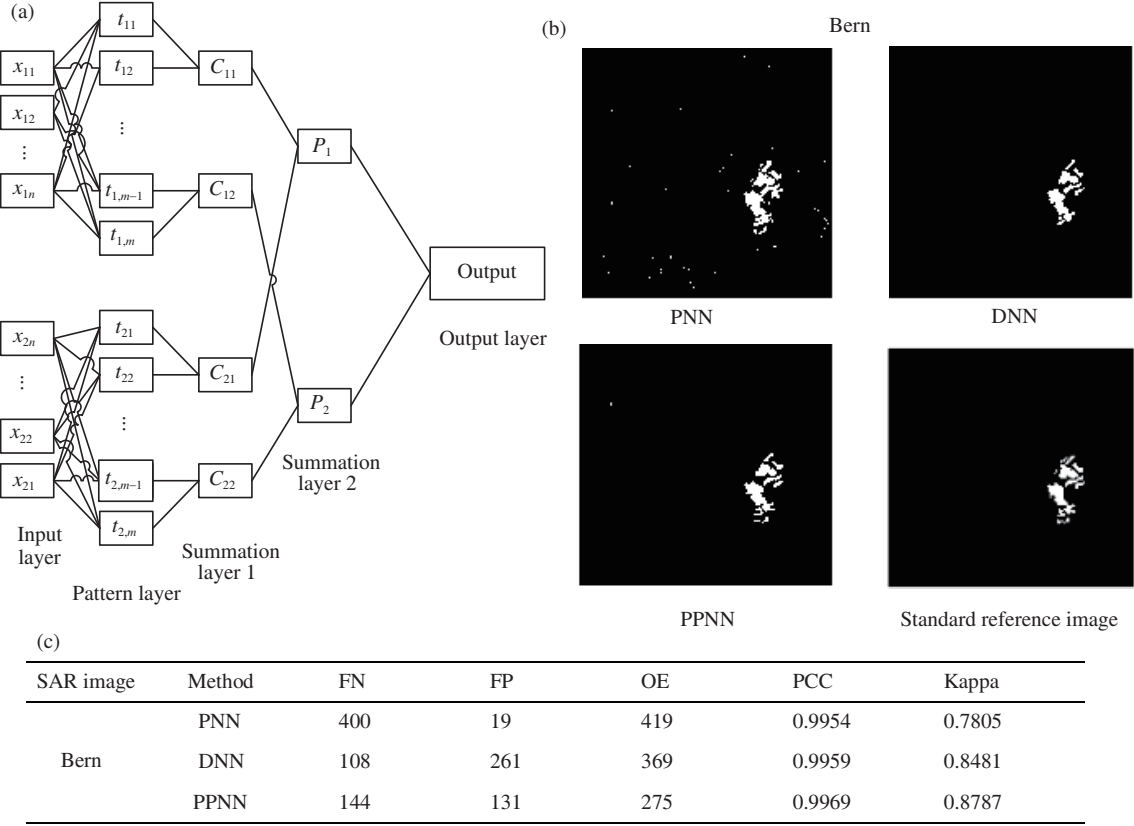


Figure 1 (a) Structure of PPNN; (b) standard reference image and the results; (c) the evaluation criteria of the results.

and

$$g(x_i) = p(W_i|x) = p(x|W_i)p(W_i) = \frac{p(W_i)}{N_i} \sum_{k=1}^{N_i} \frac{1}{(\sqrt{2\pi\sigma^2})^d} \exp\left(-\frac{\|x - x_{ik}\|^2}{2\sigma^2}\right), \quad (2)$$

where  $N_i$  is the total number of samples for category  $W_i$ ,  $d$  is the sample vector dimension,  $x_{ik}$  is the  $k$ th sample belonging to the class  $W_i$ , and  $\sigma$  is the smoothing parameter. The value of each classification function  $g_i(x)$  is obtained and inputted to the summation layer 1. For each input layer node, there will be a corresponding value in both nodes of the summation layer 1. When the four nodes of the summation layer 1 are valued, the nodes of the original PNN summation layer whose corresponding classes are located in the PPNN summation layer 1 are then weighted and summed in the summation layer 2. Finally, in the output layer, the category corresponding to the node of the summation layer 2 with a large value has an output of 1, and the category corresponding to the node with a small value has an output of 0. The final output of the network will be a binary matrix (one dimensional) corresponding to 1 and 0. This matrix is then restored in the same way to the size of the original data matrix ( $m \times n$ ), which is exactly the result of the binary image required for the final change detection.

**Results and discussion.** The set of measured SAR image data was taken by the European Remote Sensing satellite at Bern, Switzerland. The image in this data set is  $301 \times 301$  in size. The number of sample points is set to 200.

The classification results of the experiments are shown in two ways: (1) demonstrate the final change detection binary

map and (2) provide some values of the evaluation criteria to analyze the change detection results [4].

The evaluation criteria include (1) the false negative (FN), indicating the changed pixels that are undetected; (2) the false positive (FP), indicating the unchanged pixels that are wrongly classified as changed pixels; and (3) the overall error (OE) [5]. For accuracy assessment, the kappa statistic is a measure of accuracy or agreement based on the difference between the error matrix and the change agreement [6].

For the Bern dataset, this method is compared with the PNN and deep neural network (DNN) [7]. As can be seen in Figure 1(b), compared with standard references, PNN has more scattered bright points around the subject, whereas DNN has smaller scattered bright points. But DNN loses more information around the subject. As shown in Figure 1(c), the FN of PNN is 400, which is larger than the FN of DNN and PPNN, but its FP is only 19; DNN and PNN are just the opposite, which is consistent with the image. From the overall accuracy point of view, the percentage correct classification (PCC) of the PNN is 0.9954 and the kappa is 0.7805, the PCC of the DNN is 0.9959 and the kappa is 0.8481, and the PCC and kappa of PPNN are the highest at 0.9969 and 0.8787. This illustrates that compared with PNN and DNN, the accuracy of PPNN is higher.

**Conclusion.** In this study, a SAR image change detection method based on PPNN is proposed. On the one hand, this method extends the clustering problem of pixels from the point-to-point relationship to the connection between points and a set of points, which can effectively reduce the noise impact. On the other hand, it can combine the features of

different DI generation operators and calculate a comprehensive probability to classify pixels and thus improve the accuracy of change detection.

**Acknowledgements** This work was supported by National Key R&D Program of China (Grant No. 2016YFE0200400), National Natural Science Foundation of China (Grant No. 61771015), Key R&D Program of ShaanXi Province (Grant No. 2017KW-ZD-12), and Fund for Foreign Scholars in University Research and Teaching Programs (111 Project) (Grant No. B18039).

#### References

- 1 Cao X H, Ji Y M, Wang L, et al. SAR image change detection based on deep denoising and CNN. *IET Image Process*, 2019, 152: 1509–1515
- 2 Liu Y J, He J J, Ma H C, et al. Golden chip free Trojan detection leveraging probabilistic neural network with genetic algorithm applied in the training phase. *Sci China Inf Sci*, 2020, 63: 129401
- 3 Specht D F. Probabilistic neural networks. *Neural Netw*, 1990, 3: 109–118
- 4 Ma W P, Wu Y, Gong M G, et al. Change detection in SAR images based on matrix factorisation and a Bayes classifier. *Int J Remote Sens*, 2019, 40: 1066–1091
- 5 Li Y Y, Peng C, Chen Y Q, et al. A deep learning method for change detection in synthetic aperture radar images. *IEEE Trans Geosci Remote Sens*, 2019, 57: 5751–5763
- 6 Rosenfield G H, Fitzpatrick-Lins K. A coefficient of agreement as a measure of thematic classification accuracy. *Photogram Eng Remote Sens*, 1986, 52: 223–227
- 7 Keshk H M, Yin X C. Change detection in SAR images based on deep learning. *Int J Aeronaut Space Sci*, 2020, 21: 549–559